# Calibration-Free Laser-Induced Breakdown Spectroscopy (CF-LIBS): Sample Preparation for Biological Tissue

Edith Böhmer \*1,2, Laetitia S. Degelmann<sup>1</sup>, Oana-Maria Thoma<sup>3,4</sup>, Maximilian J. Waldner<sup>3,4</sup>, Florian Klämpfl<sup>1,2</sup>, Martin Hohmann<sup>1,2</sup>, and Michael Schmidt<sup>1,2</sup>

<sup>1</sup>Institute of Photonic Technologies (LPT), Friedrich-Alexander-Universität Erlangen-Nürnberg (FAU), Konrad-Zuse-Straße 3/5, 91052 Erlangen, Germany

<sup>2</sup>Erlangen Graduate School in Advanced Optical Technologies (SAOT), Paul-Gordan-Straße 6, 91052 Erlangen, Germany

<sup>3</sup>Department of Medicine 1, Friedrich-Alexander-Universität Erlangen-Nürnberg (FAU), Ulmenweg 18, 91054 Erlangen, Germany

<sup>4</sup>Germany Center for Immunotherapy, Deutsches Zentrum Immuntherapie (DZI), University Hospital Erlangen, Friedrich-Alexander-Universität Erlangen-Nürnberg (FAU), Hartmannstraße 14, 91052 Erlangen, Germany

\*Corresponding author's e-mail: edith.boehmer@fau.de

Calibration-free Laser-induced Breakdown Spectroscopy (CF-LIBS) has the significant advantage of not requiring any sample preparation, making it an attractive technique for various applications. However, to prevent sample dehydration during measurements and facilitate handling, some degree of preparation is often necessary, particularly for biological samples. The flexible structures and inherent inhomogeneity of biological tissues make it difficult to achieve optimal focus and increase the risk of elemental changes during measurement, which can adversely affect reproducibility. This study investigates the analysis of porcine skin, with the ultimate aim of applying CF-LIBS in medical contexts. The effect of embedding porcine skin samples in phosphate-buffered saline (PBS) or deionised water (dH<sub>2</sub>O) was therefore evaluated in comparison to untreated tissue. The results showed no significant differences between PBS and dH<sub>2</sub>O. However, distinct intensity deviations for magnesium and calcium were observed in embedded samples compared to untreated samples. Although embedding improves sample handling and reduces standard deviation, there may be an elemental exchange with the solution. Therefore, a careful compromise must be made between practical sample handling and potential elemental changes for any biological CF-LIBS application. This work provides valuable findings to advance CF-LIBS in biological and clinical research.

DOI: 10.2961/ilmn.2025.03.2003

**Keywords:** calibration-free Laser-induced Breakdown Spectroscopy, deionised water, elemental compostion, laser-induced Breakdown Spectroscopy, PBS, sample preparation

# 1. Introduction

A major advantage of Laser-induced Breakdown Spectroscopy (LIBS) is that it can perform elemental analysis without the need for sample preparation, making it a fast, flexible and cost-effective method [1]. This has made it very popular in areas like metallurgy, archaeology, and more and more in medicine [2-4]. In LIBS, a pulsed laser beam is focused on a solid, liquid or gaseous sample, generating a plasma through the localised ablation of the material [1]. The intense heat generated by the laser pulse rapidly vaporises the target area, breaking molecular bonds and forming a plasma containing atoms, ions and electrons originating from the sample [2]. As the plasma cools, the excited elements recombine and emit light specific to each element [5]. These emissions are collected and analysed using a spectrometer to determine the elemental composition of the sample [6].

A significant advancement in this technique is calibration-free LIBS (CF-LIBS), which enables quantitative analysis without the need for external calibration curves [4]. By fulfilling three plasma criteria, the composition of the sample can be determined from the intensity of the elements [5]. These plasma criteria include local thermodynamic equilibrium, optical thin plasma, and stoichiometric ablation, whereby the plasma composition represents that of the sample [4]. A detailed description of these criteria can be found here [5]. Ensuring these conditions are met is essential to guarantee accurate and reproducible quantification [6].

However, the quality and reproducibility of the spectra depend strongly on the laser parameters and sample-specific factors such as density, hardness, and elemental composition [1, 6]. These matrix effects can significantly impact the results, particularly in biological samples [7]. To overcome this issue, preparation methods such as drying, embedding, or freezing are employed to reduce variability and improve ablation consistency [8].

For biological tissues, which are structurally heterogeneous and compositionally complex, the impact of preparation on elemental composition remains uncertain. Since embedding media contain elemental constituents, elemental exchange with the sample is likely. This study examines how different preparation methods affect the LIBS signal, evaluating the balance between improved handling and potential changes to the elemental profile of the sample.

# 2. State of the art

Biological samples are much more difficult to handle than metals due to their heterogeneity, irregular surface structure, and poorly characterised elemental composition [4]. Depending on their physical composition, solid tissues (teeth, bones, nails), soft tissues (organs, skin) or liquid tissues (blood, mucus, urine), different preparation techniques are used [9]. These techniques are explained below.

# 2.1 Solid tissue

For hard tissues, polishing the surface can improve the interaction between the laser and the material, thereby enhancing LIBS performance [8]. To reduce matrix effects in biological samples, it is beneficial to dry, pulverise and press them into pellets, as this increases homogeneity and reproducibility [10, 11]. Nevertheless, structural modifications at the microscale may result in new spectral deviations [11].

Pulverisation aids consistent vaporisation and atomisation during plasma formation, particularly with fine powders [8]. Janovszky et al. demonstrated this by pressing pig brain tissue into pellets in order to differentiate between grey and white matter [9]. Pelletisation is also common in plant studies, for example, Jull et al. examined the effect of sodium (Na) on growth using this method [10].

# 2.2 Soft tissue

The structural heterogeneity and surface fluids (such as blood or mucus) of soft tissues can affect their optical properties, the depth of ablation and the accuracy of the results, presenting challenges for LIBS [12]. Fluids may also introduce spectral interference because the laser initially interacts with the liquid. Methods such as grids or rotating samples can improve measurement consistency [13].

In clinical settings, tissues are often embedded in paraffin for long-term preservation [14]. While this is compatible with histological staining, paraffin can cause shrinkage and protein alteration, which affects LIBS signals [14].

Epoxy resin is a more stable alternative that is widely used in the geosciences and life sciences [8, 15]. It enhances ablation efficiency due to its higher mechanical strength [15, 16]. Motto-Ros et al. [17], for instance, analysed mouse kidney tissue embedded in epoxy resin. Nevertheless, embedding media such as paraffin and epoxy resin contain elements that may alter the composition of tissue through elemental interaction.

Short-term fixation can also be achieved using a phosphate-buffered saline (PBS) solution [18]. PBS is the most commonly used buffer in immunocytochemistry and contains sodium chloride (NaCl), disodium hydrogen phosphate (Na<sub>2</sub>HPO<sub>4</sub>), potassium chloride (KCl), and potassium dihydrogen phosphate (KH<sub>2</sub>PO<sub>4</sub>) and H<sub>2</sub>O [19].

However, it should be noted that LIBS is an elemental atomic spectroscopy method, and chemical equilibration between the elements occurs as soon as a sample is embedded in a solution. Consequently, the spectrum of certain elements exhibits lower or higher intensities. The presence of salts from PBS could also introduce additional spectral lines, complicating elemental analysis and quantification. In histo-

logical practice, deionised water (dH<sub>2</sub>O) is frequently used to prepare tissue sections, particularly when smoothing and unfolding sections in a warm water bath prior to mounting on slides [20, 21]. dH<sub>2</sub>O is often used as a diluent to reduce self-absorption [8]. Self-absorption refers to the phenomenon where emitted photons from a spectral line are reabsorbed by atoms of the same element within the plasma. This results in a broadening and reduction of the line intensity, ultimately leading to an underestimation of the element's concentration in the sample [5].

Although dH<sub>2</sub>O is widely used in medical diagnostics, no studies have investigated its effect on the LIBS spectrum when used to embed biological samples. This research gap presents opportunities for future studies, particularly with regard to optimising sample preparation for LIBS analyses.

# 2.3 Fluid tissue

Pure liquids present a challenge for LIBS analysis due to surface waves, splashing and a reduced plasma lifetime, all of which degrade the quality of the measurements [21]. Freezing biological liquids such as blood or urine is an effective alternative [21]. Studies show that frozen samples can yield detection limits for magnesium (Mg) that are up to six times lower than those for liquid samples [22]. Although freezing is fast and cost-efficient, it may alter the optical properties and geometry of the sample, and this must be considered when interpreting the data.

Neverthless, none of these studies have assessed the effect of freezing on elemental composition.

# 2.4 No sample preparation

Although biological samples often require minimal preparation, several influencing factors must be considered. For example, elemental composition can vary based on patient-specific factors such as sex, age and lifestyle, as demonstrated in nail analysis by Skalny et al. [10]. Similarly, nutrition affects bone composition and postmortem shifts, such as potassium (K) loss and calcium (Ca) accumulation, occur rapidly within hours [22].

A central question is how sample preservation impacts elemental composition and consequently affects LIBS results. Additionally, it is crucial to understand compositional changes over time. This study addresses these issues by using porcine skin as a model due to its anatomical and dermal similarity to human tissue [6]. The elemental profiles of untreated samples were compared over a three-day period using two preservation methods: storage PBS or  $dH_2O$ .

The aim was to minimise sample preparation to simulate realistic, practical conditions. The evaluation criteria included changes in signal intensity, ease of measurement and sample handling, providing insights into the suitability of these preservation techniques for CF-LIBS analysis in biological research.

# 3. Materials and Methods

This study used a flashlamp-pumped, frequency-doubled, Q-switched Nd:YAG laser system (Q-Smart 450, Quantel Laser, LUMIBIRD, France), operating at a wavelength of 532 nm. This system delivers a maximum pulse energy of 150 mJ at this wavelength, with a pulse duration of 5 ns and a maximum repetition rate of 10 Hz. To adjust the laser energy more precisely, the beam path includes a polarising plate, followed by a half-wave lambda plate and a second polarising plate. After this modulation, the beam passes through a beam splitter which diverts 3.5% of the energy to an energy meter (PM100D, Thorlabs, USA) while guiding the remaining laser beam onto the sample surface. Beam focusing is achieved via a series of mirrors and a microscope objective (MY10X-823, Thorlabs, USA), which allows for the precise delivery of the laser pulse to the target. The resulting emission is collected without the use of any intermediate lenses and directed to a spectrograph (Andor Mechelle ME5000 Echelle, Oxford Instruments, UK) via an optical fibre positioned approximately 5 mm from the sample. The spectrograph offers a broad spectral range of 230-850 nm with a high spectral resolving power ( $\lambda/\Delta\lambda$ ) of 6,000, equating to a resolution of 0.1 nm at 600 nm. All measurements were conducted under ambient pressure and temperature conditions.

The experimental setup is shown in figure 1. In this study, a laser energy of 80 mJ, a delay time of 1600 ns and a gate width of 12  $\mu$ m were used, these parameters were verified in a preliminary study for CF-LIBS in porcine samples [5].

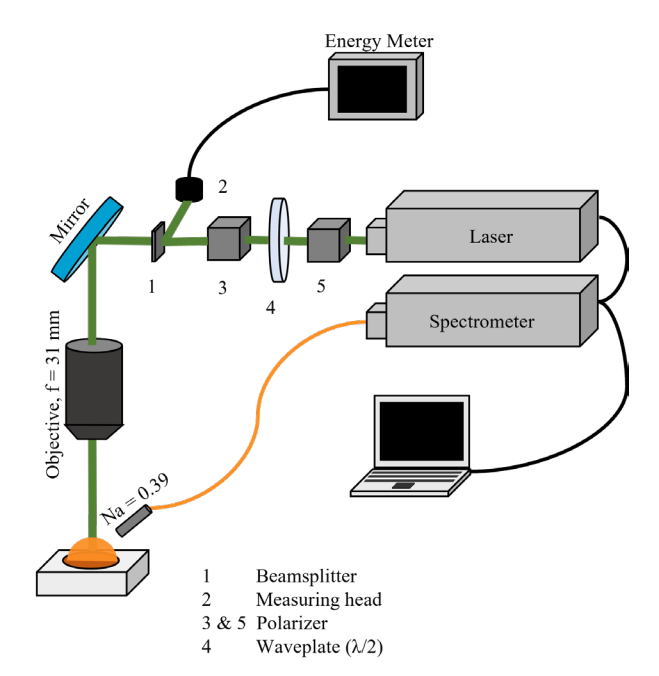


**Fig. 1** LIBS setup. The laser energy is adjusted using a measuring unit consisting of polariser and a half-wave lambda plate. A beam splitter and an energy meter measure the laser energy. The laser beam is directed at the sample surface via mirrors. The high energy of the laser beam ablates material from the surface of the sample and generates plasma. As the plasma cools, it emits light which is captured by a fibre and sent to a spectrometer. The spectrometer sends the data to a PC and generates a spectrum.

# 4. Biological samples

For this study, three porcine bellies were purchased from a local butcher. The samples from three animals have been used to reduce the effects of elemental differences due to the animals' sex, age and diet. From each porcine belly 3 skin samples per preparation method were cut by hand with a scalpel. Figure 2 shows the procine skin.



Fig. 2 Porcine skin tissue.

In order to counteract any influencing factors in the elemental reactions, an attempt was made to use approximately the same sample sizes for each tissue. All samples were weighed for this purpose. Table 1 provides an overview of the mean weights and standard deviations of the samples. After cutting the samples, they were stored separately in tubes to avoid confusion and elemental interactions.

**Table 1** Averaged weight of the samples with standard deviation.

	Weight [g]
Untreated	$0.453 \pm 0.13$
PBS	$0.552 \pm 0.12$
$dH_2O$	$0.420 \pm 0.10$

The untreated samples were placed in the refrigerator at 4 °C. The remaining samples were placed in 20 ml of PBS (PBS, pH 7.4, liquid, Sigma Aldrich, Germeny) or dH<sub>2</sub>O, and then also refrigerated at 4° C. Three spots were examined for each sample. Each spot was cleaned with a laser shot before measurement. The spot was then exposed to 10 laser shots; these were accumulated to reduce the influence of noise. After measurement, the samples were immediately cooled again to counteract any influences. Measuring a sample only takes a few minutes. All samples were packed airtight.

# 5. Element determination

PBS consists of several elements, such as Na<sub>2</sub>HPO<sub>4</sub>, KCl, NaCl and H<sub>2</sub>O. These elements can lead to elemental equilibrium between biological samples and liquid. For the evaluation of the spectra, it was decided to take the elements Mg and Ca, as it is assumed that these are only found in the biological samples and therefore diffuse only into the liquid and not from the liquid into the tissue. Na was also examined because its spectral lines were clearly identifiable in the spectrum [23]. Ca was chosen because it has well-recognisable intensities over a large wavelength range (350 nm to 650 nm) [23]. Mg was chosen because it has clear intensities in the lower wavelength range, and these lines cannot be confused with others [23]. Due to laser-material interaction, intensities between individual LIBS measurements fluctuate considerably, so intensity ratios were considered instead of individual intensities. In this study, the Na:C, Mg:C and Ca:C ratios were considered. Carbon (C) was taken as a reference because it is assumed not to change within tissue types or over time. Additionally, C does not occur in dH<sub>2</sub>O or PBS. The Na:C ratio for untreated samples and those in dH<sub>2</sub>O is used as a reference.

Several wavelengths were selected from each spectrum acording to the National Institute of Standards and Technologie (NIST) for the four elements as shown in table 2 [23]. The mean values and standard deviations of the intensities were calculated for each element at each wavelength for each generated spectrum. The intensity ratio was then calculated based on the total mean value for each element.

**Table 2** Wavelengths  $\lambda$  of the elements used to calculate the intensity ratios from NIST. With the respective upper  $E_k$  and lower energy  $E_i$  levels and transition probabilities  $g \cdot A$ , based on [23].

	$\lambda$ (nm)	$E_i$ (eV)	$E_k$ (eV)	g·A (s <sup>-1</sup> )
C	290.326	8.848	13.117	3.9· 10 <sup>6</sup>
С	290.495	8.851	13.117	6.6· 10 <sup>6</sup>
C	474.257	7.946	10.560	$3.0 \cdot 10^{5}$
C	481.216	7.480	10.056	$1.2 \cdot 10^{5}$
C	530.085	8.640	10.979	$5.7 \cdot 10^{5}$
C	580.580	8.848	10.983	$4.0 \cdot 10^{5}$
Ca	428.301	1.886	4.780	$2.1 \cdot 10^{8}$
Ca	442.544	1.900	4.680	$1.4 \cdot 10^{8}$
Ca	518.885	2.933	5.321	$2.0 \cdot 10^{8}$
Ca	526.224	2.521	4.877	$6.0 \cdot 10^{8}$
Ca	558.876	2.526	4.744	$3.4 \cdot 10^{8}$
Ca	612.200	1.886	3.910	$8.6 \cdot 10^{7}$
Ca	616.217	1.899	3.910	$1.4 \cdot 10^{8}$
Ca	649.378	2.521	4.430	$2.2 \cdot 10^{8}$
Mg	273.350	2.712	7.246	$4.6 \cdot 10^{7}$
Mg	281.111	5.946	10.355	$9.8 \cdot 10^{8}$
Mg	284.672	2.709	7.063	$3.9 \cdot 10^{7}$
Mg	291.545	5.753	10.005	$2.0 \cdot 10^{9}$
Mg	309.689	2.717	6.719	$3.4 \cdot 10^{8}$
Mg	332.992	2.709	6.431	$9.2 \cdot 10^{6}$
Mg	383.230	2.712	5.946	$6.0 \cdot 10^{8}$
Na	342.730	32.700	36.317	$1.7 \cdot 10^{8}$
Na	350.250	32.700	36.239	$3.5 \cdot 10^{8}$
Na	351.100	32.700	36.231	$3.2 \cdot 10^{8}$
Na	391.790	33.100	36.259	$5.3 \cdot 10^{8}$
Na	439.003	2.102	4.926	$3.9 \cdot 10^{6}$
Na	466.856	2.104	4.760	$1.4 \cdot 10^{7}$
Na	449.766	2.104	4.860	$8.7 \cdot 10^{6}$
Na	818.326	2.102	3.617	$1.7 \cdot 10^{8}$

#### 6. Results and Discussion

The results of the LIBS measurements are discussed below, comparing the intensity ratios of the untreated samples with the samples embeded in PBS and  $dH_2O$ .

# 6.1 Spectra

Due to the strong fluctuations in the individual LIBS spectra during the measurements, all spectra were visually inspected for noise and baseline shifts.

Each sample was measured three times, with three samples used for each preparation method and animal. This corresponds to three animals  $\cdot$  three tissues  $\cdot$  three spots = 27 spectra. This was done for one day and one preparation method. Table 3 shows how many of these spectra were ultimately used for analysis. In total,  $27 \cdot 9 = 243$  spectra were generated. Where 9 stands for three days of untreated tissue, three days of PBS and three days of dH<sub>2</sub>O. Each spectrum consists of 10 accumulated laser pulses to reduce the influence of noise.

Good spectra were identified using a combination of visual inspection and an automated Python script for spectral quality control. Initially, the script filtered out spectra with insufficient intensity, defined as the absence of peaks exceeding 1000 a.u.. This threshold was established through preliminary investigations to distinguish signal from noise. Spectra containing only a few significant spectral lines or exhibiting flat baselines, often due to misalignment or poor laser—material interaction, were excluded. Spectra with complete baseline shifts were also discarded. Following automated screening, any remaining spectra were visually reviewed to identify and exclude those with missing intensities in relevant wavelength ranges.

As shown in table 3, spectra from skin embedded in PBS produced the poorest quality results, followed by those from skin embedded in dH<sub>2</sub>O. In contrast, untreated samples consistently produced the most reliable and informative spectral profiles. Despite the fact that the embedded samples absorbed liquid over the three days, there was no clear tendency for the number of good spectra to decrease. In fact, it even increased with dH<sub>2</sub>O.

The observed increase in the number of good spectra over the three-day period may be explained by the samples gradually becoming more homogeneous due to elemental diffusion. This process probably led to more uniform surface conditions, improving the consistency of the LIBS measurements. Consequently, fluctuations between individual measurements decreased and the interaction between the laser and the sample surface became more stable and predictable.

**Table 3** Spectra used from 27 spectra generated per preparation method, divided into days 1, 2 and 3. The percentage of spectra ultimately used is shown on the left and below.

Type		Skin		[%]
Days	1	2	3	
Untreated	15	24	19	71.60
PBS	20	12	21	65.43
$dH_2O$	16	18	23	70.34
[%]	63.00	67.00	77.00	

Figure 3 shows the spectra of porcine skin compared to the sample preparation methods on day 1. The y-axis shows the intensity and the x-axis the wavelength in nm. The untreated samples are shown in red and those placed in PBS in gray, followed by the dH<sub>2</sub>O samples in yellow. In the graph, it is clearly visible that the spectral line for Na and hydrogen (H) is highest in the PBS sample. Ca is highest in the dH<sub>2</sub>O sample. In the untreated sample, only K is highest.

However for the  $dH_2O$  samples the decline is relatively small. This suggests that Na initially present in the tissue may diffuse into the embedding medium due to concentration gradients. Standard deviation remains stable in untreated samples, but decreases significantly in PBS samples. In  $dH_2O$  samples, it initially drops from day 1 to day 2 before rising again on day 3.

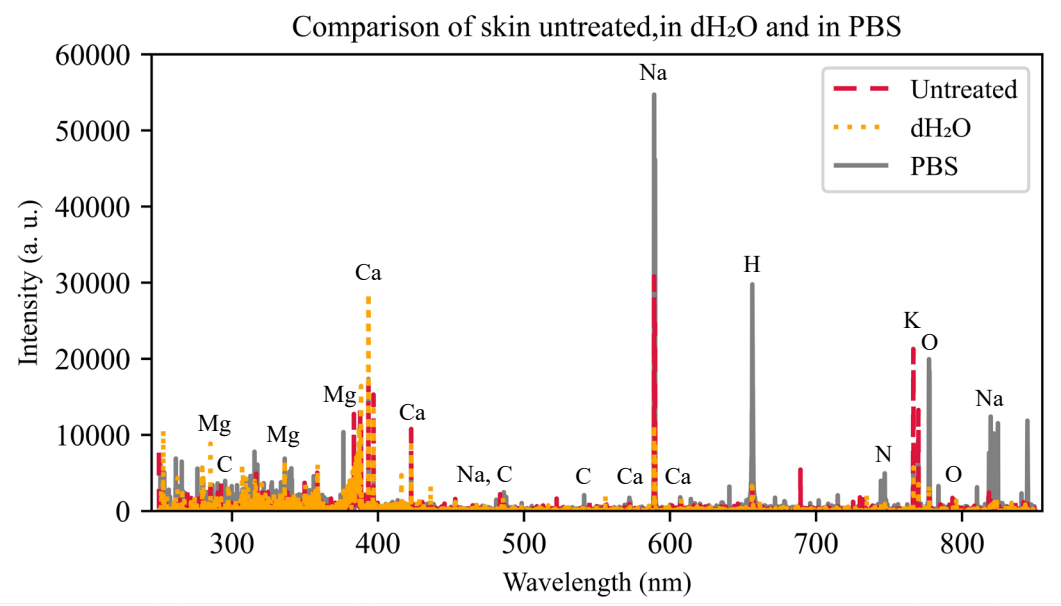


Fig. 3 LIBS spectrum of porcine skin untreated and embedded in  $dH_2O$  and PBS on day 1. For each tissue type, specific intensity peaks of certain elements are labelled. N = 27.

# 6.2 Ratio Na/C

Figure 4 shows the intensity ratio of Na to C. There is a clear trend where the mean intensity of untreated samples increases over three days, while the intensity of PBS samples decreases.  $dH_2O$  samples also show a slight increase over time. On days 1 and 2, the mean intensity of untreated and PBS samples is almost identical. However, by day 3, untreated samples clearly diverge, exhibiting higher values. Across all days,  $dH_2O$  samples consistently show the lowest mean intensities. Na levels in untreated tissue increase within the range of the standard deviation, while a decline is noted in both PBS and  $dH_2O$  embeded samples.

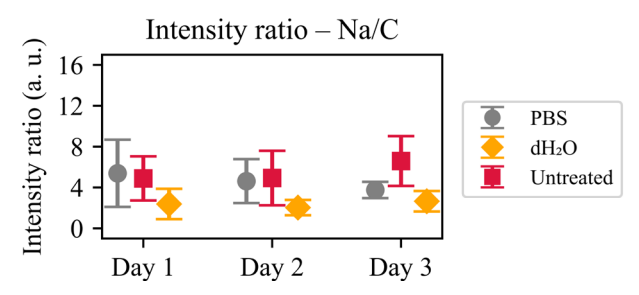


Fig. 4 Na/C ratio with standard deviation. On the x-axis are the tissue types over a period of three days. The specimens embeded into PBS are grey, those embeded into dH2O are orange and the untreated specimens are red. N=243.

# 6.3 Ratio Ca/C

The Ca/C ratio reveals more significant differences, see figure 5. Untreated samples exhibit substantially higher mean intensities and greater standard deviations than embedded samples.

Over the three-day period, both values steadily decline in untreated tissue, whereas Ca levels in PBS and dH<sub>2</sub>O remain unchanged. Initially, PBS samples show slightly higher values than dH<sub>2</sub>O samples, but this relationship reverses by day 3. In both embedding conditions, a decrease in standard deviation is observed, indicating a stabilising effect over time. The consistent values suggest that the amount of Ca present in the samples and in the fluids is the same, while its concentration in untreated tissue decreases within the range of the standard deviation.

Direct comparisons are difficult due to the limited literature currently available on the elemental distribution of Ca and related elements in different tissue types. Nevertheless, it is generally assumed that Ca is naturally present in relatively high concentrations in skin tissue. As neither  $dH_2O$  nor PBS contains Ca, immersion in these media is likely to promote diffusion-driven elemental exchange. Consequently, Ca may diffuse from the tissue into the surrounding solution during treatment, resulting in a lower Ca concentration in the embedded samples than in untreated tissue.

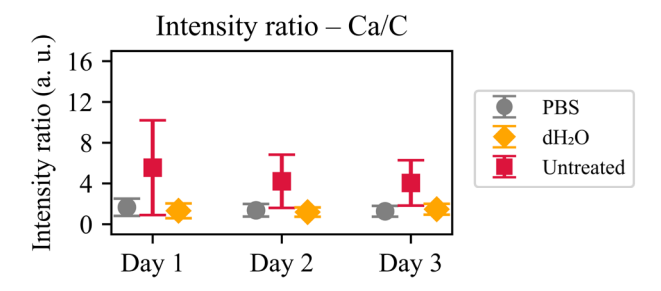


Fig. 5 Ratio of Ca to C intensities with standard deviation. Tissue samples over a period of three days are shown on the x-axis. The samples placed in PBS are shown in grey, the samples placed in  $dH_2O$  are shown in orange and the untreated samples are shown in red. The intensity ratio is plotted on the y-axis. N=243.

# 6.4 Ratio Mg/C

The difference between untreated and embedded samples is particularly notable in the Mg/C ratio as shown in Fig. 6. Untreated samples exhibit a notably higher mean intensity, approximately 5 a.u. higher, than embedded porcine skin samples. The Mg intensity in untreated samples decreases by day 2, rising slightly by day 3 within the margin of the standard deviation, which remains constant across all days. In contrast, both PBS and dH<sub>2</sub>O samples show a continuous decline in mean intensity and standard deviation over time. As Mg is not a component of either embedding solution, its reduction can be attributed to diffusion from the tissue into the surrounding medium. This observation supports the idea that embedding solutions can change the elemental composition of biological samples by facilitating selective element exchange.

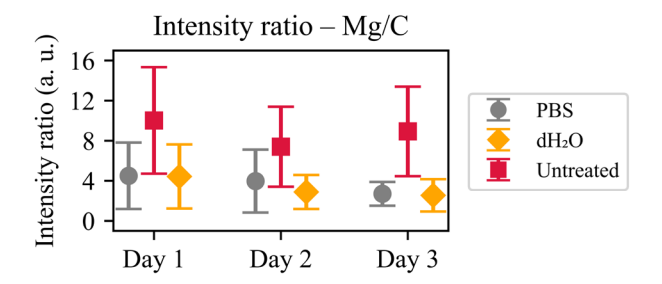


Fig. 6 Intensity ratio of Mg to C with the standard deviation. The x-axis shows the respective tissue samples over a period of three days. In gray the samples put in PBS, in orange the samples put in  $dH_2O$  and in red the untreated samples. The intensity ratio is plotted on the y-axis. N=243.

# 7. Limitation

To counteract biological influences on the porcine samples, such as age, sex, and diet, as much as possible, porcine samples from three animals were used. However, the butcher did not have more precise data on these animals, such as origin, sex, or time of slaughter. The LIBS spectra were analysed at three different locations in order to reduce the variance. Due to the flexible structure of the samples, it was not possible to cut them with a vibratome, so the samples were cut with a scalpel, resulting in non-palnar surfaces. This non-

planar surface can cause the laser to be slightly out of focus, resulting in lower spectrum intensities.

Due to the hand-cutting of the samples, samples of different sizes were cut for each tissue type. An attempt was made to keep the weight similar.

# 8. Discussion

To ensure accurate and reproducible LIBS measurements, particularly in the context of calibration-free analysis, special attention must be paid to the choice of embedding medium. Although PBS and dH<sub>2</sub>O had similar effects on spectral profiles, they both differed notably from untreated tissue, particularly with regard to the Ca/C ratio. This highlights the necessity of first comparing embedding media with untreated tissue for each tissue type and elemental ratio in order to evaluate potential matrix effects and elemental interactions.

Such interactions arise from the tendency of elements to reach equilibrium in terms of concentration between the tissue and the surrounding fluid. As demonstrated in Jansen et al.'s [22] study, postmortem elemental shifts can occur, including an increase in Na concentrations across various rat organs shortly after death. Jansen et al. [22] also observed an initial decrease in K, followed by a secondary increase, which he attributed to its release into the extracellular space due to cellular breakdown and subsequent protein degradation. Similarly, Nagaraj et al. [24] reported elevated Ca levels in goats following slaughter, which were likely caused by Ca leakage triggered by the denaturation of intracellular regulatory proteins. Both researchers noted a subsequent decline in these elemental concentrations, although the mechanisms behind this reversal remain unclear. By contrast, while this study identified no significant increase in Ca, primarily due to a lack of precise slaughter time information, there was a clear secondary rise in both Mg and Na. Further investigation is required to determine how such elemental changes manifest in different tissue types.

# 9. Conclusion

This study provides a thorough evaluation of the impact of embedding in PBS or dH<sub>2</sub>O on the spectral characteristics of porcine skin. It was demonstrated that immersion had no significant effect on the overall spectral quality compared to untreated tissue. Minor variations were primarily observed in the Na/C and Mg/C ratios for skin, while general intensity and reproducibility remained consistent across all conditions. Therefore, it is essential to analyse LIBS samples as soon as possible to minimise the influence of changes in elemental composition over time. These results are significant because they confirm that extensive sample preparation is unnecessary, thus preserving the rapid and straightforward nature of LIBS analysis.

# Acknowledgments

The authors would like to express their gratitude to Fanuel Mehari for their valuable contributions to the scientific discourse. The authors gratefully aknowledge funding of the Erlangen Graduate School in Advanced Optical Technologies (SAOT) by the Bavarian State Ministry for Science and Art. The aurhors would like to thank the German Resarch Foundation (DFG- Deutsche Forschungsgemeinschaft) for its support. This work was achieved in the context of the

DFG-project "Calibration-free Laser-induced Breakdown Spectroscopy (LIBS) for the elemental analysis of tissue" (502911968).

# Declaration of generative AI and AI-assisted technologies

During the preparation of this work the authors used "DeepL Write" in order to improve language and readability. After using this tool, the authors reviewed and edited the content as needed and take full responsibility for the content of the publication.

# **Conflicts of Interest**

The authors declare no conflicts of interest.

#### References

- [1] E. Asamoah and Y. Hongbing: J. Appl. Phys., 123, (2017), 22
- [2] N. Hausmann: "Laser-induced Breakdown Spectroscopy (LIBS) in der Archäologie", (Arch. Inf., Mainz, 2024), p. 1.
- S. Maurice, R. C. Wiens, P. Bernardi, P. Caïs, S. Robinson, T. Nelson, O. Gasnault, J. M. Reess, M. Deleuze, F. Rull, J.-A. Manrique, S. Abbaki, R. B. Anderson, Y. André, S. M. Angel, G. Arana, T. Battault, P. Beck, K. Benzerara, S. Bernard, J.-P. Berthias, O. Beyssac, M. Bonafous, B. Bousquet, M. Boutillier, A. Cadu, K. Castro, F. Chapron, B. Chide, K. Clark, E. Clavé, S. Clegg, E. Cloutis, C. Collin, E. C. Cordoba, A. Cousin, J.-C. Dameury, W. D'Anna, Y. Daydou, A. Debus, L. Deflores, E. Dehouck, D. Delapp, G. de Los Santos, C. Donny, A. Doressoundiram, G. Dromart, B. Dubois, A. Dufour, M. Dupieux, M. Egan, J. Ervin, C. Fabre, A. Fau, W. Fischer, O. Forni, T. Fouchet, J. Frydenvang, S. Gauffre, M. Gauthier, V. Gharakanian, O. Gilard, I. Gontijo, R. Gonzalez, D. Granena, J. Grotzinger, R. Hassen-Khodja, M. Heim, Y. Hello, G. Hervet, O. Humeau, X. Jacob, S. Jacquinod, J. R. Johnson, D. Kouach, G. Lacombe, N. Lanza, L. Lapauw, J. Laserna, J. Lasue, L. Le Deit, S. Le Mouélic, E. Le Comte, Q.-M. Lee, C. Legett, R. Leveille, E. Lewin, C.Leyrat, G. Lopez-Reyes, R. Lorenz, B. Lucero, J. M. Madariaga, S. Madsen, M. Madsen, N. Mangold, F. Manni, J.-F. Mariscal, J. Martinez-Frias, K. Mathieu, R. Mathon, K. P. McCabe, T. McConnochie, S. M. McLennan, J. Mekki, N. Melikechi, P.-Y. Meslin, Y. Micheau, Y. Michel, J. M. Michel, D. Mimoun, A. Misra, G. Montagnac, C. Montaron, F. Montmessin, J. Moros, V. Mousset, Y. Morizet, N. Murdoch, R. T. Newell, H. Newsom, N. Nguyen Tuong, A. M. Ollila, G. Orttner, L. Oudda, L. Pares, J. Parisot, Y. Parot, R. Pérez, D. Pheav, L. Picot, P. Pilleri, C. Pilorget, P. Pinet, G. Pont, F. Poulet, C. Quantin-Nataf, B. Quertier, D. Rambaud, W. Rapin, P. Romano, L. Roucayrol, C. Royer, M. Ruellan, B. F. Sandoval, V. Sautter, M. J. Schoppers, S. Schröder, H.-C. Seran, S. K. Sharma, P. Sobron, M. Sodki, A. Sournac, V. Sridhar, D. Standarovsky, S. Storms, N. Striebig, M. Tatat, M. Toplis, I. Torre-Fdez, N. Toulemont, C. Velasco, M. Veneranda, D. Venhaus, C. Virmontois, M. Viso, P. Willis, and K. W. Wong: Space Sci. Rev., 213, (2021), 1

- [4] D. A. Cremers and L. J. Radziemski: "Handbook of laser-induced breakdown spectroscopy", (A John Wiley & Sons Ltd Publication, Chichester, 2013), p. 31.
- [5] E. Böhmer, L. S. Degelmann, D. Ni, F. Klämpfl, and M. Schmidt: Proc. SPIE INt. Soc. Opt. Eng., 13317, (2025), 18
- [6] F. Mehari: "Laser-induced Breakdown Spectroscopy (LIBS) as a diagnostics tool for biological tissue analysis", (FAU University Press, Erlangen, 2023), p. 24.
- [7] M. Müller: "Neue Wege zur Quantifizierung mit der laserinduzierten Plasmaspektroskopie: (LIBS)", (BAM-Dissertationsreihe, Berlin, 2010), p. 30.
- [8] S. C. Jantzi, V. Motto-Ros, F. Trichard, Y. Markushin, N. Melikechi, and A. de Giacomo: Spectrochim. Acta, Part B, 115 (2016), 52
- [9] P. Janovszky, A. Kéri, D., J. Palásti, L. Brunnbauer, F. Domoki, A. Limbeck, and G. Galbács: Sci. Rep., 13, (2023), 10089
- [10] H. Jull, R. Kunnemeyer, S. Talele, P. Schaare, and M. Seelye: Int. J. Intell. Rob. Appl., 6, (2015), 262
- [11] C. Sun, W. Xu, Y. Tan, Y. Zhang, Z. Yue, L. Zou, S. Shabbir, M. Wu, F. Chen, and J. Yu: Sci. Rep., 11, (2021), 21379
- [12] F. Mehari, M. Rohde, C. Knipfer, R. Kanawade, F. Klämpfl, W. Adler, F. Stelzle, and M. Schmidt: Biomed. Opt. Express, 5, (2014), 4013
- [13] M. Ogura, S. Sato, M. Ishihara, S. Kawauchi, T. Arai, T. Matsui, A. Kurita, M. Kikuchi, H. Ashida, and M. Obara: Lasers Surg. Med., 31, (2002), 136
- [14] A. W. Benecke: "Etablierung eines Verfahrens zur histologischen Analyse humaner Hornhäute unter besonderer Beachtung der Descemet-Membran und des kornealen Endothels", (University Press, Hamburg, 2009), p. 20.
- [15] S. Moncayo, F. Trichard, B. Busser, M. Sabatier-Vincent, F. Pelascini, N. Pinel, I. Templier, J. Charles, L. Sancey, and V. Motto-Ros: Spectrochim. Acta, Part B B, 133, (2017), 40
- [16] L. Bush: "LIBS at the Submicrometer Scale", (Spectroscopy, Berkeley, 2016), p. 1.
- [17] L. Sancey, V. Motto-Ros, B. Busser, S. Kotb, J. M. Benoit, A. Piednoir, F. Lux, O. Tillement, G. Panczer, and J. Yu: Sci. Rep., 4, (2014), 6065
- [18] B. Chazotte: "Labeling Golgi with fluorescent ceramides", (Cold Spring Harbor protocols, New York, 2012), p. 3.
- [19] J. Sambrook and D. W. Russell: "Molecular cloning: A laboratory manual", (Cold Spring Harbor Laboratory Press, Cold Spring Harbor, 2001), p. 3.
- [20] C. Flössel, T. Luther, M. Müller, S. Albrecht, and M. Kasper: Histochem., 101, (1994), 449
- [21] G. Lang: "Histotechnik: Praxislehrbuch für die Biomedizinische Analytik", (Springer, Vienna, 2013), p. 285.
- [22] H. H. Jansen: "Der Kalium-, Natrium- und Wassergehalt der inneren Organe zu bestimmten Zeiten nach dem Tode", (Virchows Arch. path Anat., Kiel, 1961), p. 510.
- [23] A. Kramida, Y. Ralchenko, J. Reader, and NIST ASD Team, NIST Atomic Spectra Database (2025).

[24] N. S. Nagaraj, K. R. Anilakumar, and K. Santhanam: J. Muscle Foods, 17, (2006), 198

(Received: June 5, 2025, Accepted: September 28, 2025)